

Effects of solvents and metal ions on the synthesis, structural diversity and magnetic properties of 5'-nitro-[1,1':3',1''-terphenyl]-3,3'',5,5''-tetracarboxylic acid ligand and a highly sensitive sensor for Fe³⁺

Yuan-Yu Yang,^a Jian-Hua Xue,^a Dong-Dong Yang,^{*a} Li-Yang Zhang,^a Qi Ma^{*a} and Xuan Zhao^{*b}

^a College of Chemistry and Chemical Engineering, Shanxi Datong University, Datong 037009, P. R. China. E-mail: ddyang@sxdtdx.edu.cn; maqihx@163.com.

^b Department of Chemistry, Key Laboratory of Bioorganic Phosphorus Chemistry & Chemical Biology, Tsinghua University, Beijing 100084, P. R. China. E-mail: zhaox0320@mail.tsinghua.edu.cn

CONTENTS

Fig. S1 The IR spectra of H₄nttba ligand and complexes **1-4**.

Fig. S2 (a) View of the single 2D framework of complex **1**. (b) The void size of the 2D framework of complex **1**

Fig. S3 The void size of the 2D framework of complex **2**.

Fig. S4 The void size of the 2D framework of complex **3**.

Fig. S5 PXRD patterns of complexes **1-4** at room temperature.

Fig. S6 The thermal curves of complexes **1-4**.

Fig. S7 The solid-state emission spectra of complex **4** and H₄nttba at room temperature.

Fig. S8 The emission spectra of complex **4** in different solvents.

Fig. S9 The PXRD patterns of simulated complex **4**, the PXRD patterns of **4** for the recognition of Fe³⁺ after five recycling processes.

Fig. S10 Liquid U - vis spectra of complex **4**, Fe³⁺ in the solution.

Table S1 Selected bond distances (Å) and angles (°) for **1**, **2**, **3** and **4**.

Table S2. A comparison of selected MOFs-based luminescent sensors for the detection of Fe³⁺ ion.

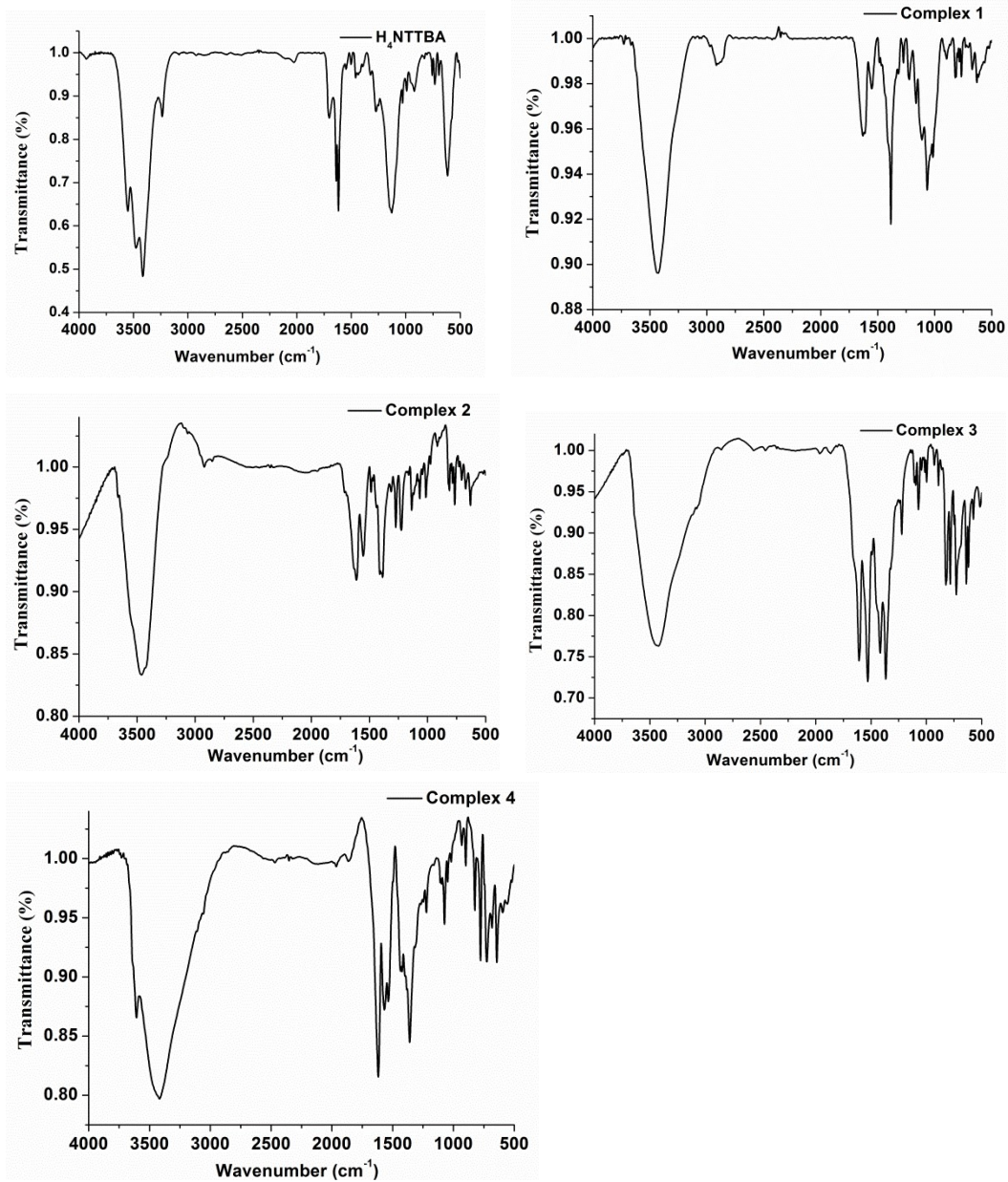


Fig. S1 The IR spectra of H_4nttba ligand and complexes 1-4.

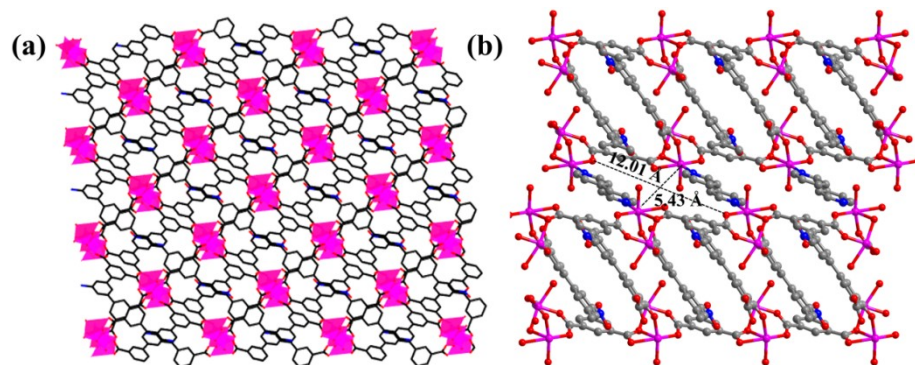


Fig. S2 (a) View of the single 2D framework of complex 1. (b) The void size of the 2D

framework of complex 1.

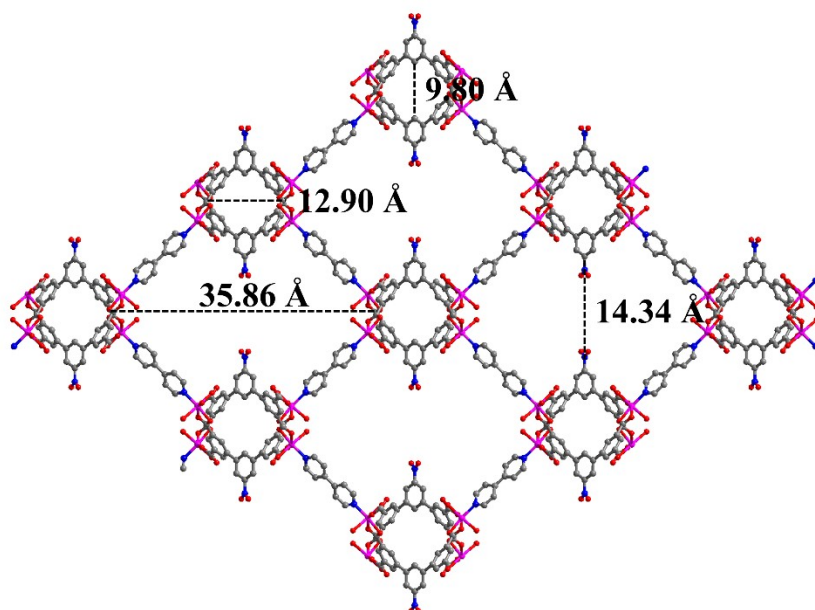


Fig. S3 The void size of the 2D framework of complex 2.

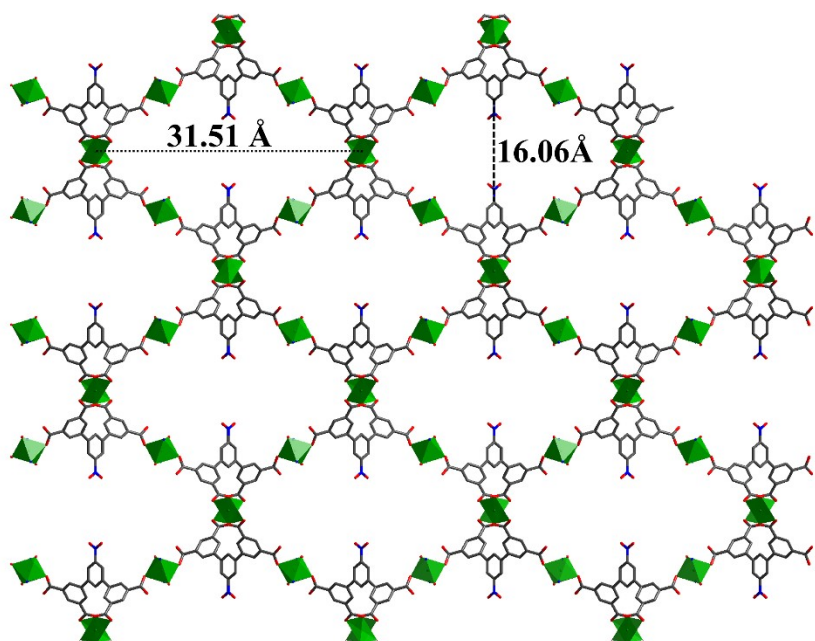


Fig. S4 The void size of the 2D framework of complex 3.

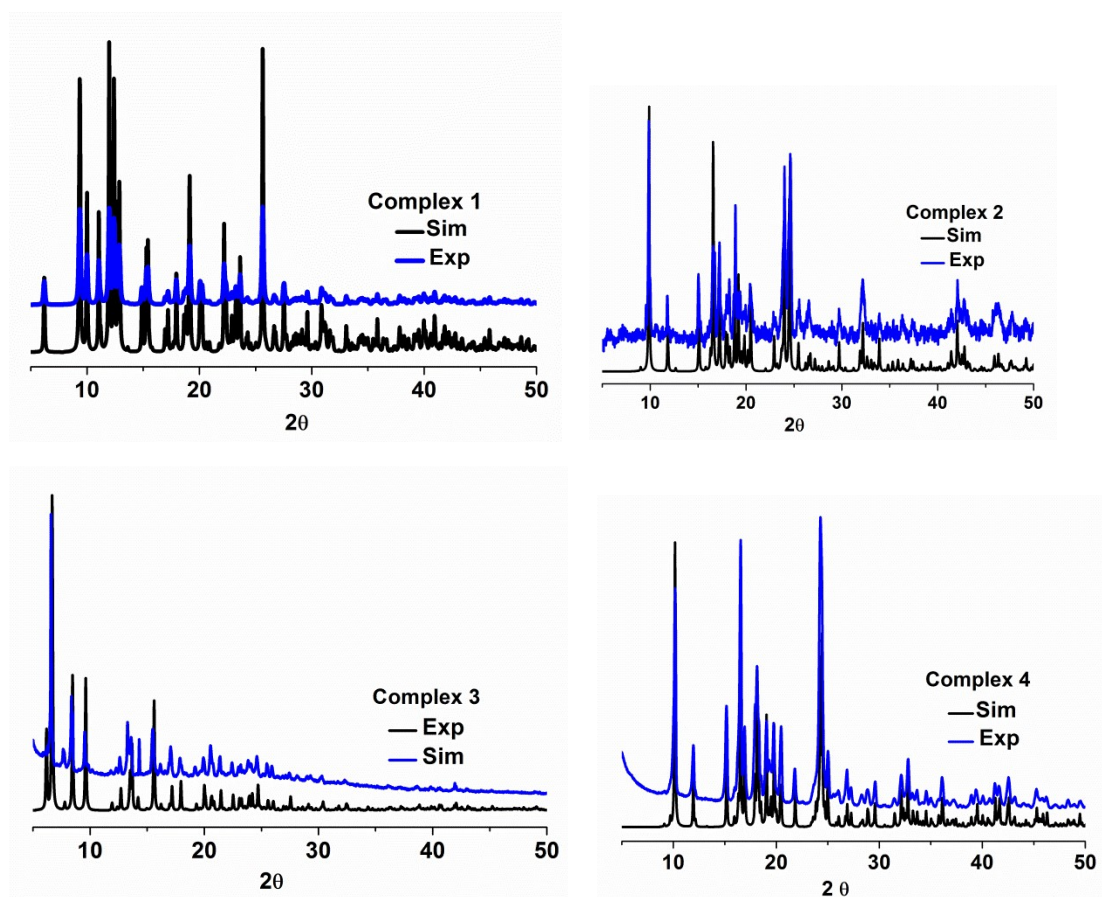


Fig. S5 PXRD patterns of complexes 1–4 at room temperature. Blue patterns correspond to the experimental data obtained using the as synthesized bulk samples. Black patterns were simulated from the single crystal X-ray data.

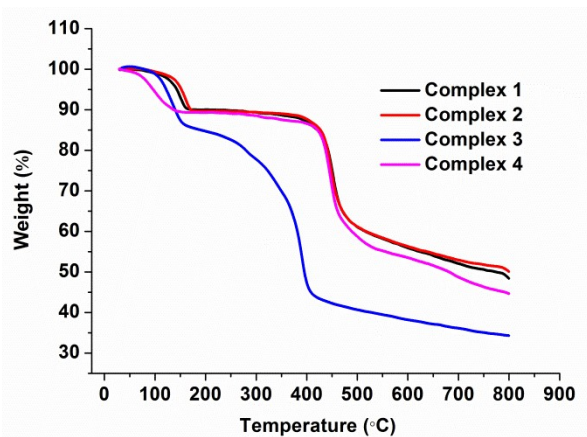


Fig. S6 The thermal curves of complexes 1-4.

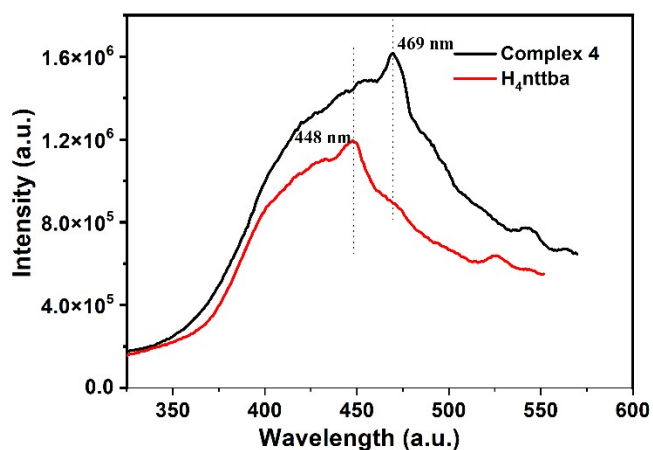


Fig. S7 The solid-state emission spectra of complex 4 and H₄nttba at room temperature.

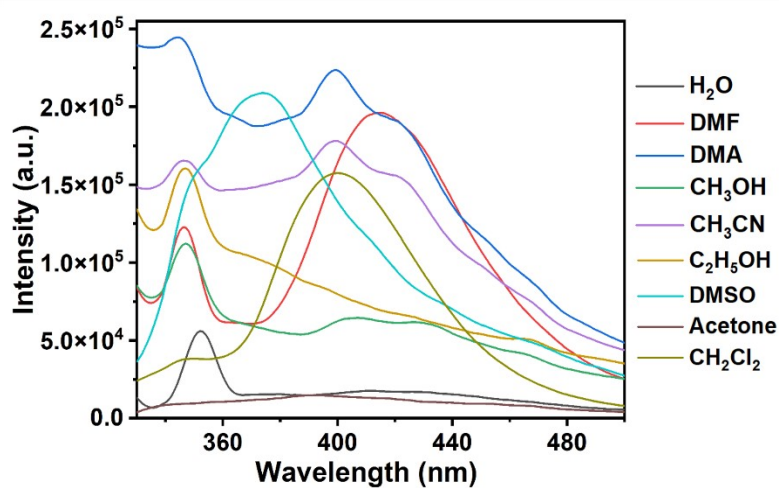


Fig.S8 The emission spectra of complex 4 in different solvents.

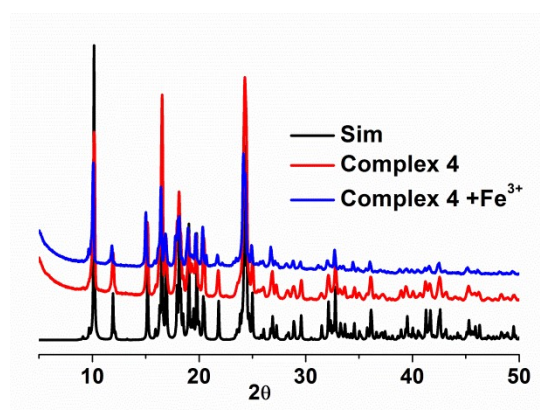


Fig. S9 The PXRD patterns of simulated complex 4, the PXRD patterns of 4 for the recognition of Fe³⁺ after five recycling processes.

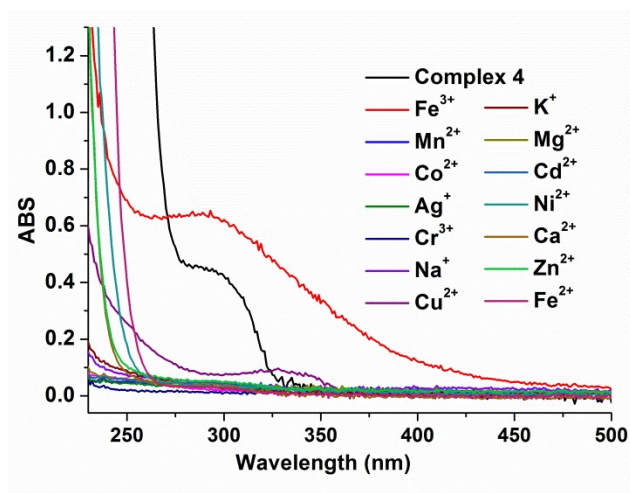


Fig. S10 Liquid U - vis spectra of complex **4** , Fe³⁺ in the solution.

Table S1 Selected bond distances (Å) and angles (°) for **1**, **2**, **3** and **4**.

Complex 1			
Co1—O8 ⁱ	2.050 (3)	Co2—O7	1.896 (3)
Co1—N2	2.084 (3)	Co2—O1 ⁱⁱⁱ	1.954 (3)
Co1—O3 ⁱⁱ	2.086 (3)	Co2—O4 ^{iv}	1.963 (3)
Co1—O11	2.134 (3)	Co2—O9 ^v	2.124 (3)
Co1—O9	2.165 (3)	Co2—O12	2.262 (7)
Co1—O10	2.258 (3)		
O8 ⁱ —Co1—N2	95.94 (12)	O3 ⁱⁱ —Co1—O11	168.71 (13)
O8 ⁱ —Co1—O3 ⁱⁱ	105.73 (13)	O8 ⁱ —Co1—O9	100.32 (10)
N2—Co1—O3 ⁱⁱ	88.61 (12)	N2—Co1—O9	163.65 (11)
O8 ⁱ —Co1—O11	85.56 (13)	O3 ⁱⁱ —Co1—O9	88.67 (11)
N2—Co1—O11	90.60 (12)	O11—Co1—O9	88.93 (12)
O8 ⁱ —Co1—O10	157.31 (11)	O7—Co2—O1 ⁱⁱⁱ	108.91 (15)
N2—Co1—O10	104.59 (11)	O7—Co2—O4 ^{iv}	124.15 (17)
O3 ⁱⁱ —Co1—O10	84.62 (12)	O1 ⁱⁱⁱ —Co2—O4 ^{iv}	120.64 (15)
O11—Co1—O10	84.69 (12)	O7—Co2—O9 ^v	92.97 (13)
O9—Co1—O10	59.10 (9)	O1 ⁱⁱⁱ —Co2—O9 ^v	111.61 (14)
O4 ^{iv} —Co2—O9 ^v	91.56 (13)	O4 ^{iv} —Co2—O12	81.3 (2)
O7—Co2—O12	74.5 (2)	O9 ^v —Co2—O12	158.1 (3)
O1 ⁱⁱⁱ —Co2—O12	89.7 (3)		

Complex 2			
Co1—O1	2.021 (2)	Co1—O7	2.121 (3)
Co1—O4 ⁱ	2.060 (3)	Co1—O6	2.162 (3)
Co1—N2	2.067 (3)	Co1—O3 ⁱ	2.277 (3)
O1—Co1—O4 ⁱ	95.50 (11)	O1—Co1—O6	87.16 (12)
O1—Co1—N2	98.42 (12)	O4 ⁱ —Co1—O6	91.09 (13)
O4 ⁱ —Co1—N2	165.92 (12)	N2—Co1—O6	87.50 (13)
O1—Co1—O7	92.83 (11)	O7—Co1—O6	177.68 (12)
O4 ⁱ —Co1—O7	91.22 (13)	O1—Co1—O3 ⁱ	155.38 (11)
N2—Co1—O7	90.21 (13)	O4 ⁱ —Co1—O3 ⁱ	60.47 (10)
N2—Co1—O3 ⁱ	105.46 (11)	O6—Co1—O3 ⁱ	87.97 (12)
O7—Co1—O3 ⁱ	92.98 (12)		
Complex 3			
Ni1—O6 ⁱ	2.0484 (12)	Ni2—N1 ⁱⁱ	2.0537 (15)
Ni1—O6	2.0485 (12)	Ni2—N1 ⁱⁱⁱ	2.0537 (15)
Ni1—O4	2.0705 (11)	Ni2—O2	2.0943 (12)
Ni1—O4 ⁱ	2.0705 (11)	Ni2—O2 ^{iv}	2.0944 (12)
Ni1—N2	2.1219 (14)	Ni2—O1 ^{iv}	2.1283 (13)
Ni1—N2 ⁱ	2.1220 (14)	Ni2—O1	2.1284 (13)
O6 ⁱ —Ni1—O6	180.0	O4—Ni1—O4 ⁱ	180.00 (6)
O6 ⁱ —Ni1—O4	87.87 (5)	O6 ⁱ —Ni1—N2	90.21 (5)
O6—Ni1—O4	92.13 (5)	O6—Ni1—N2	89.79 (5)
O6 ⁱ —Ni1—O4 ⁱ	92.14 (5)	O4—Ni1—N2	89.33 (5)
O6—Ni1—O4 ⁱ	87.87 (5)	O4 ⁱ —Ni1—N2	90.67 (5)
O6 ⁱ —Ni1—N2 ⁱ	89.79 (5)	N1 ⁱⁱ —Ni2—O2	96.21 (6)
O6—Ni1—N2 ⁱ	90.21 (5)	N1 ⁱⁱⁱ —Ni2—O2	100.67 (5)
O4—Ni1—N2 ⁱ	90.68 (5)	N1 ⁱⁱ —Ni2—O2 ^{iv}	100.67 (5)
O4 ⁱ —Ni1—N2 ⁱ	89.32 (5)	N1 ⁱⁱⁱ —Ni2—O2 ^{iv}	96.21 (6)
N2—Ni1—N2 ⁱ	180.0	O2—Ni2—O2 ^{iv}	156.16 (7)
N1 ⁱⁱ —Ni2—N1 ⁱⁱⁱ	89.51 (9)	N1 ⁱⁱ —Ni2—O1 ^{iv}	162.90 (5)
N1 ⁱⁱⁱ —Ni2—O1 ^{iv}	92.15 (6)	N1 ⁱⁱⁱ —Ni2—O1	162.90 (5)

O2—Ni2—O1 ^{iv}	100.20 (5)	O2—Ni2—O1	62.23 (5)
O2 ^{iv} —Ni2—O1 ^{iv}	62.23 (5)	O2 ^{iv} —Ni2—O1	100.20 (5)
N1 ⁱⁱ —Ni2—O1	92.15 (6)	O1 ^{iv} —Ni2—O1	91.25 (8)
Complex 4			
Zn1—O4 ⁱ	1.948 (3)	Zn1—O6	2.156 (4)
Zn1—O2	1.966 (3)	Zn1—O7	2.248 (4)
Zn1—N2	2.020 (3)		
O4 ⁱ —Zn1—O2	104.06 (15)	O4 ⁱ —Zn1—O7	89.34 (16)
O4 ⁱ —Zn1—N2	149.22 (15)	O2—Zn1—O7	88.22 (15)
O2—Zn1—N2	106.04 (15)	N2—Zn1—O7	85.34 (15)
O4 ⁱ —Zn1—O6	92.81 (17)	O6—Zn1—O7	175.61 (15)
O2—Zn1—O6	94.96 (14)	N2—Zn1—O6	90.86 (15)

Table S2. A comparison of selected MOFs-based luminescent sensors for the detection of Fe³⁺ ion.

MOFs and related materials	Analyte	K _{sv} (M ⁻¹)	Detection Limit (mol/L)	Ref
Eu ³⁺ @MIL-124	Fe ³⁺	3.874×10 ⁴	2.8×10 ⁻⁷	S1
NTU-9-NS(Ti)	Fe ³⁺	-	4.5×10 ⁻⁷	S2
[Cd ₂ (L)(bimid)(DMF) ₂](DMF)	Fe ³⁺	3.75×10 ⁴	3.70×10 ⁻⁷	S3
Eu-BPDA	Fe ³⁺	1.25×10 ⁴	9×10 ⁻⁷	S4
{Cd ₃ ·L ⁶ ·(BTB) ₂ ·2DMF} _n	Fe ³⁺	1.01 × 10 ⁴	1.12 × 10 ⁻⁶	S5
Eu ₂ (OH-BDC) ₃	Fe ³⁺	-	1.17×10 ⁻⁶	S6
{[Cd(L) _{0.5}](1,8-NDC) · H ₂ O]} _n	Fe ³⁺	7.75 × 10 ³	1.40 × 10 ⁻⁶	S7
[Zn(L)(bpe)]·DMF	Fe ³⁺	2.27×10 ⁴	1.55×10 ⁻⁶	S8
BUT-14	Fe ³⁺	2.17×10 ³	3.8×10 ⁻⁶	S9
[Zn ₂ (cptpy)(btc)(H ₂ O)] _n	Fe ³⁺	5.456×10 ³	4.33×10 ⁻⁶	S10
{[Zn(NTTBA) _{0.5} (4,4'-bpy) _{0.5} (H ₂ O) ₂].0.5H ₂ O} _n	Fe ³⁺	5.05×10 ³	6.96 × 10 ⁻⁶	This work
[Tb(BTB)(DMF)]·1.5DMF·2.5H ₂ O	Fe ³⁺	-	1×10 ⁻⁵	S11
{[Zn ₂ (BIBP) ₂ (HL) ₂] · 2H ₂ O} _n	Fe ³⁺	2.21 × 10 ⁴	2.29 × 10 ⁻⁵	S12
FJI-C8 (Zn)	Fe ³⁺	8245	2.33×10 ⁻⁵	S13
[Cd(Hcbic)] _n	Fe ³⁺	1.8×10 ⁵	3.1×10 ⁻⁵	S14
[Eu(atpt) _{1.5} (phen)(H ₂ O)] _n	Fe ³⁺	7.60×10 ³	4.5×10 ⁻⁵	S15
{[Zn(L ¹)(dcdps)]} _n	Fe ³⁺	7.004 × 10 ³	6.21 × 10 ⁻⁵	S16
{Zn(L ¹)(bdc)} _n	Fe ³⁺	9.066 × 10 ³	4.45 × 10 ⁻⁵	S16

[Zn ₅ (hfipbb) ₄ (trz) ₂ (H ₂ O) ₂]	Fe ³⁺	4.1×10 ⁵	1.8×10 ⁻⁴	S17
[Ln(μ ₃ -cpta)(phen)(H ₂ O) ₂]n	Fe ³⁺	2138	2.0×10 ⁻⁴	S18
HPU-1 (Zn)	Fe ³⁺	1.0 × 10 ⁴	1.09 × 10 ⁻³	S19

- Xu, X.-Y.; Yan, B., Eu(III)-Functionalized MIL-124 as Fluorescent Probe for Highly Selectively Sensing Ions and Organic Small Molecules Especially for Fe(III) and Fe(II). *ACS Appl. Mater. Interface* **2014**, *7* (1), 721-729.
- Zhou, L.; Zhao, K.; Hu, Y.-J.; Feng, X.-C.; Shi, P.-D.; Zheng, H.-G., A bifunctional photoluminescent metal–organic framework for detection of Fe³⁺ ion and nitroaromatics. *Inorg Chem Commun* **2018**, *89*, 68-72.
- Xu, H.; Gao, J.; Qian, X.; Wang, J.; He, H.; Cui, Y.; Yang, Y.; Wang, Z.; Qian, G., Metal–organic framework nanosheets for fast-response and highly sensitive luminescent sensing of Fe³⁺. *J. Mater. Chem. A* **2016**, *4* (28), 10900-10905.
- Wang, J.; Wang, J.; Li, Y.; Jiang, M.; Zhang, L.; Wu, P., A europium(iii)-based metal–organic framework as a naked-eye and fast response luminescence sensor for acetone and ferric iron. *New J Chem* **2016**, *40* (10), 8600-8606.
- Fan, M.; Sun, B.; Li, X.; Pan, Q.; Sun, J.; Ma, P.; Su, Z., Highly Fluorescent Cadmium Based Metal–Organic Frameworks for Rapid Detection of Antibiotic Residues, Fe³⁺ and Cr₂O₇²⁻ Ions. *Inorg. Chem.*, **2021**, *60* (12), 9148-9156.
- Xu, H.; Dong, Y.; Wu, Y.; Ren, W.; Zhao, T.; Wang, S.; Gao, J., An -OH group functionalized MOF for ratiometric Fe³⁺ sensing. *J Solid State Chem* **2018**, *258*, 441-446.
- Shi, Y.-S.; Li, Y.-H.; Cui, G.-H.; Dong, G.-Y., New two-dimensional Cd(ii) coordination networks bearing benzimidazolyl-based linkers as bifunctional chemosensors for the detection of acetylacetone and Fe³⁺. *CrystEngComm* **2020**, *22* (5), 905-914.
- Chen, Z.; Mi, X.; Wang, S.; Lu, J.; Li, Y.; Li, D.; Dou, J., Two novel penetrating coordination polymers based on flexible S-containing dicarboxylate acid with sensing properties towards Fe³⁺ and Cr₂O₇²⁻ ions. *J Solid State Chem* **2018**, *261*, 75-85.
- Wang, B.; Yang, Q.; Guo, C.; Sun, Y.; Xie, L.-H.; Li, J.-R., Stable Zr(IV)-Based Metal–Organic Frameworks with Predesigned Functionalized Ligands for Highly Selective Detection of Fe(III) Ions in Water. *ACS Appl. Mater. Interface* **2017**, *9* (11), 10286-10295.
- Chen, H.; Fan, P.; Tu, X.; Min, H.; Yu, X.; Li, X.; Zeng, J. L.; Zhang, S.; Cheng, P., A Bifunctional Luminescent Metal–Organic Framework for the Sensing of Paraquat and Fe³⁺ Ions in Water. *Chem. Asian J.*, **2019**, *14* (20), 3611-3619.
- Xu, H.; Hu, H.-C.; Cao, C.-S.; Zhao, B., Lanthanide Organic Framework as a Regenerable Luminescent Probe for Fe³⁺. *Inorg. Chem.*, **2015**, *54* (10), 4585-4587.
- Xue, Y.-S.; Zhang, C.; Lv, J. Q.; Chen, N.-N.; Wang, J.; Chen, X.-R.; Fan, L., Luminescence sensing and photocatalytic activities of four Zn(ii)/Co(ii) coordination polymers based on a pyridinephenyl bifunctional ligand. *CrystEngComm* **2021**, *23* (6), 1497-1506.
- Chen, C.-H.; Wang, X.-S.; Li, L.; Huang, Y.-B.; Cao, R., Highly selective sensing of Fe³⁺ by an anionic metal–organic framework containing uncoordinated nitrogen and carboxylate oxygen sites. *Dalton Trans.*, **2018**, *47* (10), 3452-3458.
- Li, F.-F.; Zhu, M.-L.; Lu, L.-P., A luminescent Cd(II)-based metal–organic framework for detection of

Fe(III) ions in aqueous solution. *J Solid State Chem* **2018**, *261*, 31-36.

15. Kang, Y.; Zheng, X.-J.; Jin, L.-P., A microscale multi-functional metal-organic framework as a fluorescence chemosensor for Fe(III), Al(III) and 2-hydroxy-1-naphthaldehyde. *J Colloid Interface Sci* **2016**, *471*, 1-6.

16. Ge, F.-Y.; Sun, G.-H.; Meng, L.; Ren, S.-S.; Zheng, H.-G., Four New Luminescent Metal–Organic Frameworks as Multifunctional Sensors for Detecting Fe³⁺, Cr₂O₇²⁻ and Nitromethane. *Cryst. Grow. Des.*, **2019**, *20* (3), 1898-1904.

17. Gu, J.-Z.; Cai, Y.; Liu, Y.; Liang, X.-X.; Kirillov, A. M., New lanthanide 2D coordination polymers constructed from a flexible ether-bridged tricarboxylate block: Synthesis, structures and luminescence sensing. *Inorg. Chim. Acta* **2018**, *469*, 98-104.

18. Li, H.; He, Y.; Li, Q.; Li, S.; Yi, Z.; Xu, Z.; Wang, Y., Highly sensitive and selective fluorescent probe for Fe³⁺ and hazardous phenol compounds based on a water-stable Zn-based metal–organic framework in aqueous media. *RSC Adv.* **2017**, *7* (79), 50035-50039.

19. Zhao, X.-L.; Tian, D.; Gao, Q.; Sun, H.-W.; Xu, J.; Bu, X.-H., A chiral lanthanide metal–organic framework for selective sensing of Fe(III) ions. *Dalton Trans.*, **2016**, *45* (3), 1040-1046.